Defence Science Journal, Vol. 75, No. 2, March 2025, pp. 257-262, DOI : 10.14429/dsj.19978

Dynamic Analysis of FG Shaft with SMA Supports

K. Udayanand

DRDO-Naval Science Technological Laboratory, Visakhapatnam - 530 027, India
E-mail: kudayanand.nstl@gov.in

ABSTRACT

Vibration control has been given paramount importance in industries and defence applications for the efficient functioning of all rotating machinery and to minimize vibration transmission. In defence applications, a significant percentage of vibration is contributed by rotating and reciprocating machinery. The vibration of machinery is crucial from a stealth perspective. Since vibration results in structure-borne sound power, it is predominantly transmitted to a sound-carrying structure from a source via multiple contact points to the underwater environment, leading to the detection of ships and submarines. Consequently, noise and vibrations propagate through the structure, potentially causing sensitive equipment to vibrate or generate undesired radiated noise. The resultant vibration levels of heavy-duty and high-capacity machinery are higher compared to low-capacity machines. In principle, the magnitude of vibration can be reduced through measures at the source, during transmission, while propagating, or at radiation. The machinery parts that significantly affect overall vibration can be reengineered to introduce controls at the source. A concept of Functional Graded Material (FGM) can be proposed for the shafts of machines to reduce overall vibration by varying the material composition based on a gradient index (K) and providing damping in the system. This concept yields effective results when implemented in thermal environments, such as the engine compartments of ships and submarines. The main advantage of using FGMs instead of traditional materials is that the internal composition of their component materials can be tailored to meet the requirements of a specific structure. FGMs are increasingly important as designers seek ways to address structures under combined mechanical and thermal loads. Similarly, vibration levels can be reduced by implementing measures in the transmission path. However, in real systems, the maximum damping is limited and cannot be arbitrarily increased in the resonance region. In such scenarios, Shape Memory Alloys (SMAs) are potential candidates for controlling vibrations by varying stiffness, particularly in applications requiring large amounts of force. Therefore, a rotor system utilizing Functionally Graded Materials (FGM) for the shaft and shape memory alloys for the bearing support structure is evaluated to assess the effective control of both resonances (shifting the critical speeds). In many countries, various isolation methods are employed to reduce the vibration levels transmitted to the structures of underwater vessels. This paper attempts to study the vibration and stability analyses of FG shafts with SMA supports based on the finite element method.

Keywords: Functional graded material; Shape memory alloy; Stability; Internal damping; Power law; Campbell diagram

1. INTRODUCTION

Functionally Graded Material (FGM) is characterised by a gradual variation in composition and structure throughout its volume. Due to the resulting properties of FGMs, such as high strength, high stiffness, low density, and good damping characteristics, Functional Graded (FG) shafts have emerged as promising candidates for replacing conventional shafts in various applications involving the design of rotating mechanical components. Nelson and McVaughn described the dynamics of rotor-bearing systems using finite elements[1], incorporating the effects of rotary inertia, gyroscopic moments, and shear deformation. Zorzi and Nelson[2] studied the finite element simulation of rotor-bearing systems while considering damping. Chang et al.[3] modeled a simple spinning composite shaft by employing the three-dimensional constitutive relations of the material through extended Hamilton's principle. Rao and Roy[4] conducted a dynamic analysis of an FG rotor system with a three-disc rotor shaft using Timoshenko beam theory. Boukhalfa[5] highlighted the impact of various material combinations in FGMs on natural frequencies. However, in real-time systems, the maximum damping is limited and cannot be arbitrarily increased in the resonance region. Shape memory alloys (SMAs) have been utilised as potential candidates for both light and heavy-duty equipment to control vibrations.

These SMAs can facilitate safe coasting of the rotor past critical speeds at high acceleration rates, thereby reducing large resonant vibrations. Gupta[6], *et al.* investigated resonance control of rotors using shape memory alloys. In this study, structural components in the form of support springs made of shape memory alloy were employed in the rotor support to mitigate resonance conditions by utilizing the properties of SMAs. Enemark[7], *et al.* conducted experiments to examine the effects of shape memory alloys on the dynamics of rotor-bearing systems. Yong-Yong He[8], *et al.* investigated the vibration control of a rotor–bearing system utilizing SMAs in the pedestal bearing.

Received : 16 April 2024, Revised : 27 October 2024
Accepted : 22 November 2024, Online published : 24 March 2025

2. OBJECTIVES AND SCOPE

This study aims to perform dynamic analysis of an FG shaft supported by SMA, and the scope of this work includes (i) examining the influence of the power law gradient index on the variation of mechanical properties of the FG shaft across the radial direction of the material and various vibration parameters of the shaft. (ii) Finite modeling of different combinations of the FG shaft to conduct dynamic analysis. (iii) Investigating the resonance control of the rotor using SMA and designing & developing an experimental setup for the FG shaft with SMA springs.

3. MODELING OF FG SHAFT WITH SMA SPRING SUPPORTS

Dynamic analysis of the FG shaft with bearing pedestals supported on SMA springs is illustrated in Fig. 1. Initially, the dynamic analysis of the FG shaft with SMA at room temperature is conducted, and the dynamic analysis of the FG shaft with SMAs in both activated and deactivated states is performed to examine the combined effective resonance control and unbalanced response of the rotor system using both FG shaft and SMA materials. This analysis also aims to compare the vibration parameters of the FG shaft alone.

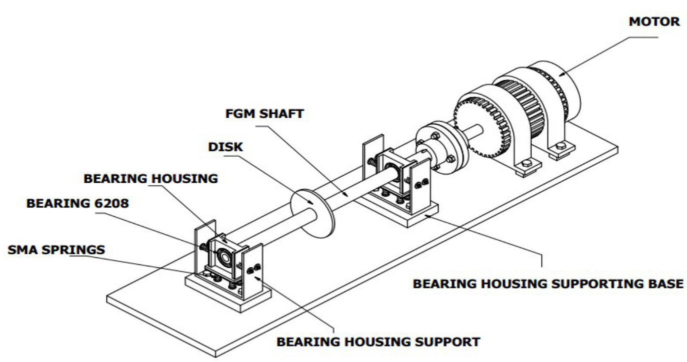

Figure 1. FG Shaft with SMA Spring Supports.

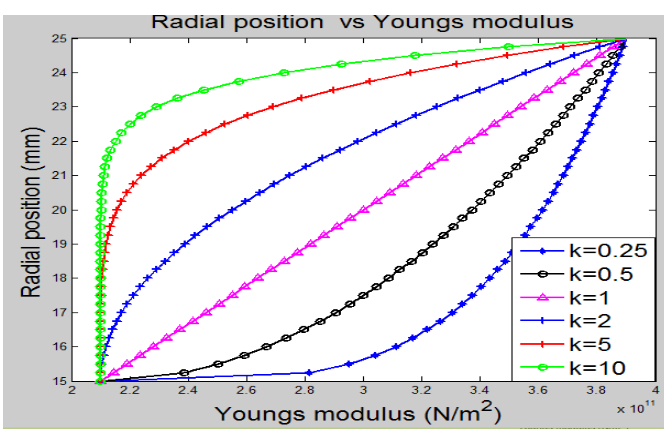

Figure 2. Effect of power law gradient index on young's modulus of FGM.

3.1 Estimation of Properties of FG Shaft

Since FGM is a heterogeneous material, selecting the optimal volume fraction of the two materials is crucial for achieving the best performance of rotating machinery.

There are two methods for estimating the properties at each layer throughout the thickness of the FG shaft: (i) Exponential gradation law and (ii) Power law gradation. The power law gradation provides an accurate estimation of the properties of each layer of the FGM shaft. An FGM shaft with a finite length 'L', an outer radius r_c, and an inner radius r_m is considered for this work. According to the power law,

$$v_c(z) = \left(\frac{r - rm}{rc - rm}\right)^K \tag{1}$$

Property of FG material at any radius 'z' can be obtained from

$$P(z) = \{P_C(z) - P_m(z)\} V_C(z) + P_m(z) \tag{2}$$

A combination of FGM (steel – Al_2O_3) has been examined to illustrate the effect of gradient index (K) on mechanical properties such as density and Poisson's ratio at various radial positions with K. A typical graph showing the variation of Young's modulus with radial position[9] is presented in Fig. 2.

3.2 Governing Equations of FG Shaft with SMA Supports

The FG shaft is modeled as a Timoshenko beam based on first-order shear deformation theory (FOSD), accounting for the gyroscopic effect and rotary inertia of the shaft. The hollow rotor shaft is assumed to rotate at a constant speed along the longitudinal axis. The rotor-bearing systems consist of a disc, FG finite shaft elements, and discrete bearings with Nitinol springs. A schematic FE model of the FG shaft with bearings and Nitinol (SMA) springs, along with coordinate systems, is shown in Fig. 3, where K_B and K_{SMA} represent bearing stiffness and the effective stiffness of the SMA springs, respectively. CB denotes bearing damping. The shaft is analysed by discretizing it into 12 three-noded beam elements, resulting in a total of 25 nodes, each with 4 degrees of freedom. The disc is positioned in the middle of the shaft.

The Strain energy of FG shaft can be obtained as follows:

$$U_S = \frac{1}{2} \mathrm{v}\int \left(\sigma_{xx}\,\varepsilon_{xx} + 2\tau_{xr}\varepsilon_{xr} + 2\tau_{x\theta}\,\varepsilon_{x\theta}\right) dV \tag{3}$$

The kinetic energy of FG shaft (T_s) and disc during T_d rotation can be written as:

$$T_s = \frac{1}{2}\int_0^L \left[I_m\left(\dot{v}_0^{2} + \dot{W}_0^{2}\right) + I_d\left(\dot{\beta}_x^{2} + \dot{\beta}_y^{2}\right) - 2\Omega I_p \beta_x \dot{\beta}_y^{2} + \Omega^2 I_d\left(\beta_X^2 + \beta_y^2\right) + \Omega^2 I_p \right] dx$$

$$T_d = \frac{1}{2}\int_0^L \sum_{i=1}^{N_D} \left[I_{mi}^D\left(\dot{v}_0^{2} + \dot{W}_0^{2}\right) + I_{di}^D\left(\dot{\beta}_x^{2} + \dot{\beta}_y^{2}\right) - 2\Omega I_{pi}^D \beta_x \dot{\beta}_y^{2} + \Omega^2 I_{pi}^D \right] \Delta\left(x - x_{Di}\right) dx$$

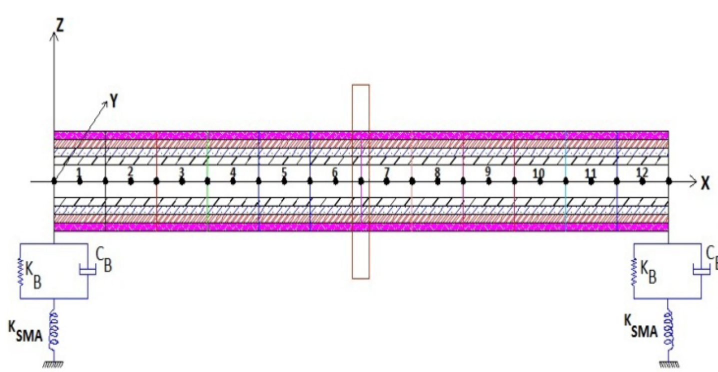

Figure 3. FE model of FG shaft with rigid disc mounted on SMA supports.

Work done due to external loads, bearings and SMA springs can be obtained as follows:

$$\delta W_E = \int_0^L \left(Q_y \delta v_0 + Q_z \delta w_0 + M_y \delta B_y + M_x \delta B_x \right) dx \tag{4}$$

$$\delta W_B = \int_0^L \sum_{i=1}^{N_B} \begin{pmatrix} -K_{yy}^{i} v_0 \delta v_0 - v_0 \delta w_0 - K_{yz}^{Bi} w_0 \delta v_0 - K_{zz}^{i} w_0 \delta w_0 \\ -C_{yy}^{Bi} \dot{v}_0 \delta v_0 - C_{zy}^{Bi} \dot{v}_0 \delta w_0 - C_{yz}^{Bi} \dot{w}_0 \delta v_0 - C_{zz}^{Bi} \dot{w}_0 \delta w_0 \end{pmatrix} \Delta\left(-x_{Bi}\right) dx \tag{5}$$

(K_{yy}^{i}) is addition of bearing stiffness (K_{yy}^{Bi}) and stiffness of SMA (K_{SMA}^{i}) when it is activated /deactivated in series.

By taking the strain energy of shaft, the kinetic energy of the shaft and disc, and the work done into account and invoking the Hamilton's principle, which is

$$\int_{t1}^{t2} \left[\delta T - \delta U_s + \delta W_E + \delta W_B \right] dt = 0 \tag{6}$$

Here, the total kinetic energy of the system is K.E of shaft and disc $T = T_s + T_d$ and the material for the disc is considered isotropic material.

Therefore

$$\int_{t1}^{t2} \left[\delta\left(T_s + T_d\right) - \delta U_s + \delta W_E + \delta W_B \right] dt = 0 \tag{7}$$

The equations of motion can be obtained from the above expression.

$$\delta v_0 : I_m \frac{\partial^2 v_0}{\partial t^2} + k_s \left(A_{55} + A_{66}\right)\left(\frac{\partial \beta_y}{\partial x} - \frac{\partial^2 v_0}{\partial x^2}\right) + \frac{1}{2} k_s A_{16} \frac{\partial^2 \beta_x}{\partial x^2} + \sum_{i=1}^{N_D} I_m^D \frac{\partial^2 v_0}{\partial t^2} \triangle\left(x - x_{Di}\right) + F_{v_o}^b = Q_y$$

$$\delta w_0 : I_m \frac{\partial^2 w_0}{\partial t^2} - k_s \left(A_{55} + A_{66}\right)\left(\frac{\partial^2 w_0}{\partial x^2} - \frac{\partial \beta_x}{\partial x}\right) + \frac{1}{2} k_s A_{16} \frac{\partial^2 \beta_y}{\partial x^2} + \sum_{i=1}^{N_D} I_m^D \frac{\partial^2 w_0}{\partial t^2} \triangle\left(x - x_{Di}\right) + F_{w_o}^b = Q_z$$

$$\partial \beta_x \grave{U} I_d \frac{\partial^2 \beta_x}{\partial t^2} - I_p \quad \frac{\partial \beta_y}{\partial t} + \frac{1}{2} k_s A_{16} \frac{\partial^2 v_0}{\partial x^2} - B_{11} \frac{\partial^2 \beta_x}{\partial x^2} - k_s \left(A_{55} + A_{66}\right)\left(\frac{\partial w_0}{\partial x} + \beta_x\right) + \sum_{i=1}^{N_D} \left(I_{di}^D \frac{\partial^2 \beta_x}{\partial t^2} - \quad I_{pi}^D \frac{\partial \beta_y}{\partial t} \right) \triangle\left(x - x_{Di}\right) = M_x$$

$$\partial \beta_y \grave{U} I_d \frac{\partial^2 \beta_y}{\partial t^2} - I_p \Omega \frac{\partial \beta_x}{\partial t} + \frac{1}{2} k_s A_{16} \frac{\partial^2 w_0}{\partial x^2} - B_{11} \frac{\partial^2 \beta_y}{\partial x^2} - k_s \left(A_{55} + A_{66}\right)\left(\beta_x - \frac{\partial v_0}{\partial x}\right) + \sum_{i=1}^{N_D} \left(I_{di}^D \frac{\partial^2 \beta_y}{\partial t^2} - \quad I_{pi}^D \frac{\partial \beta_x}{\partial t} \right) \triangle\left(x - x_{Di}\right) = M_y \tag{8}$$

Where

$$F_{v_o}^b = \sum_{j=1}^{N_B} \left(K_{yy}^{i} v_0 + K_{yz}^{Bi} w_0 + C_{yy}^{Bi} \dot{v}_0 + C_{yz}^{Bi} \dot{w}_0 \right) \text{ and}$$

$$F_{v_o}^b = \sum_{j=1}^{N_B} \left(K_{zz}^{i} w_0 + K_{zy}^{Bi} v_0 + C_{zz}^{Bi} \dot{w}_0 + C_{zy}^{Bi} \dot{v}_0 \right)$$

By applying Hemelton's principle and substituting the expressions for the displacement variables into the governing equations, the Lagrangian equations of motion can be formulated for the finite element of the rotating FG shaft depicted in Fig. 3 as follows.

$$[M]\left\{\ddot{q}\right\} + [D]\{\dot{q}\} + [K]\{q\} = \{F\} \tag{9}$$

where, matrices [M] and [K] are mass and stiffness respectively. [D] Matrix consists of damping and gyroscopic matrices. {q} and {f} represents nodal displacement and external force vectors respectively. Considering the unbalance of disc only, force for the equation of motion in the form of

$$\{F\} = \{F_C\} cos\Omega t + \{F_S\} sin\Omega t \tag{10}$$

A steady-state solution of the same form is assumed as

$$\{q\} = \{a\} cos\Omega t + \{b\} sin\Omega t \tag{11}$$

This Eqn. substituted in equation of motion which yields

$$\begin{Bmatrix} \{q_c\} \\ \{q_s\} \end{Bmatrix} = \begin{bmatrix} K - \Omega^2 [M] & -\Omega^2 [G] \\ \Omega^2 [G] & K - \Omega^2 [M] \end{bmatrix}^{-1} \begin{Bmatrix} \{F_c\} \\ \{F_s\} \end{Bmatrix} \tag{12}$$

which provides undamped system unbalanced response. Critical speeds can be calculated from Eigen frequencies of the system

$$\begin{bmatrix} [0] & [M] \\ [M] & [D] \end{bmatrix} \{\dot{h}\} - \begin{bmatrix} -[M] & [0] \\ [0] & [K] \end{bmatrix} \{h\} = \{H\}_{8nX1} \tag{13}$$

Assume a solution form, $\{h\} = \{h_0\} e^{\lambda t}$ for the above homogeneous equation of motion. Eigenvalue problem is

$$\begin{bmatrix} [0] & [I] \\ -[K]^{-1}[M] & -[K]^{-1}[D] \end{bmatrix} \{h\} = \frac{1}{\lambda} \{h_0\} \tag{14}$$

and complex eigenvalues of the system are determined in the form $\alpha_i = \lambda_i + j\omega_i$ in which real part (λ) represents system damping. The imaginary part of the Eigen value will give the system natural whirl frequency.

4. DYNAMIC ANALYSIS OF FG SHAFT

Dynamic analysis of the FG shaft is conducted to examine various parameters, including natural frequencies, unbalanced responses, critical speeds, and stability aspects. A MATLAB program has been developed based on the governing equations to compare these parameters of the shaft.

4.1 Problem Specifications of FG Shaft

The material selected for the conventional shaft system, including both the shaft and disc, is steel. It features a hollow rotor shaft with inner and outer diameters of 0.03 m and 0.05 m, respectively, and a length of 1 m. additionally, it includes a disc with a diameter of 0.2 m and a thickness of 0.03 m, positioned with an eccentricity of 3×10^{-5}m. The shaft is supported by two identical orthotropic bearings that have been modeled. The operating speed of the shaft is 3500 rpm (366.67 rad/sec). The stiffness and damping coefficients for each bearing at both ends are defined as $K_{yy} = 7 \times 10^5$ N/m, $K_{zz} = 5 \times 10^5$ N/m, $C_{yy} = 700$ Ns/m and $C_{zz} = 500$ N/m. The bearing pedestals are supported by four vertical and four horizontal SMA springs within the bearing housing, with the stiffness of each spring at room temperature being 1630.5 N/m.

4.2 Comparison of Natural Frequencies and Unbalance Responses

Every system has its own natural frequencies, and if the frequency of the disturbing force is close to any of these natural frequencies, the amplitude can increase significantly. This phenomenon is known as resonance. Therefore, it is

Table 1. Natural Frequencies and Unbalance Response of Steel & FG Shaft

Material	Natural frequencies (rad/s)	Unbalance response (μm)
	Mode 1	
Steel	361.90	526.7
Al+Steel	367.98	899.7
Steel+Al	255.03	462.9
SiC+Steel	428.89	289.3
Steel+SiC	411.03	236.8
Ni+Steel	354.16	530.7
Steel+Ni	365.75	531.3
Steel+Al_2O_3	442.11	93.17
Al_2O_3+Steel	409.77	263.29

crucial to determine the natural frequency of the system. The natural frequencies of various FG combinations, such as Aluminium-steel, SiC-steel, Nickel-steel, and steel-Al_2O_3, are presented in Table 1. This table indicates that the FG shaft with a combination of Steel and Al_2O_3 exhibits higher natural frequencies compared to other FG combinations and the steel shaft.

Rotor dynamic characteristics, such as unbalanced response behaviour, have been given paramount importance in the life cycle of rotor systems. From the results of unbalanced response amplitudes of various FG combinations at the disc location, it can be understood that, except for the steel-nickel and steel-aluminium combinations, all other combinations will result in a reduction of amplitude levels compared to those of the conventional rotor.

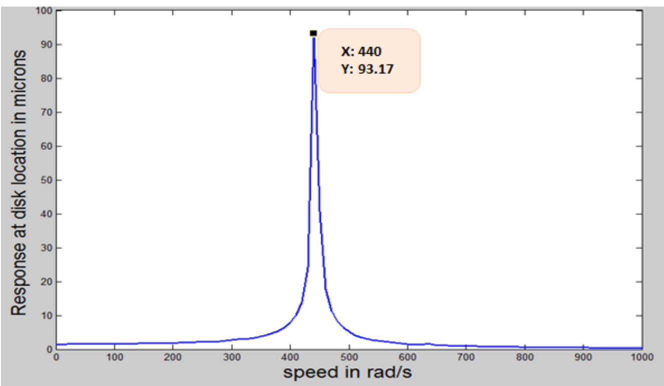

Figure 4. Unbalance response of FG shaft.

The combination of FG materials in the inner and outer layers also influences the response of the FG shaft. The pairing of FG material steel with Al_2O_3 as the outer layer yields the lowest result (see Fig. 4). When considering damping, it is noted that the critical speed shifts towards higher values.

4.3 Comparative Study of Critical Speeds and Stability Aspects

Critical speeds of a shaft can be obtained from the Campbell diagram. Campbell diagrams plotted for conventional and FG rotors are shown in Fig. 5.

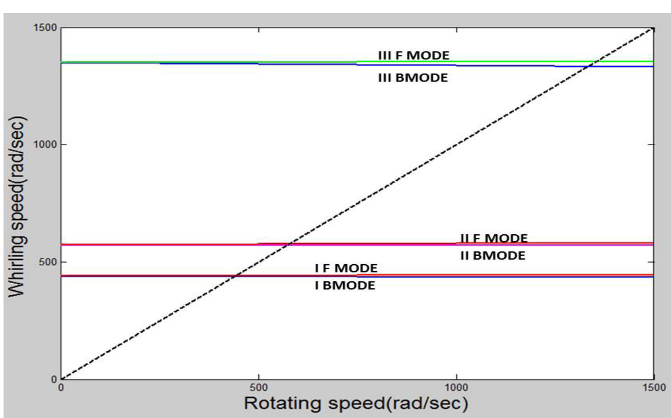

Figure 5. Campbell diagram of FG shaft.

The labels 'F' and 'B' in the figures refer to the forward and backward modes, respectively.

The first critical speed for the conventional shaft occurs in the forward mode at 362.18 rad/s, while for the FG shaft, the critical speed is at 447.53 rad/s. Additionally, it is noted that with the influence of damping, the first critical speed is at 464.65 rad/s. Stability analysis is conducted by examining the real parts of complex eigenvalues derived from a complex eigenvalue analysis. The complex eigenvalues of the system are determined in the form [11].

$$\alpha_i = \lambda_i + j\omega_i \tag{15}$$

The real part represents the damping exponent of the system, and the rotor is considered stable if it is negative. Stability diagrams are compared and plotted for conventional and FG rotor systems based on the real part of complex eigenvalues, as illustrated in Fig. 6 and Fig. 7, respectively.

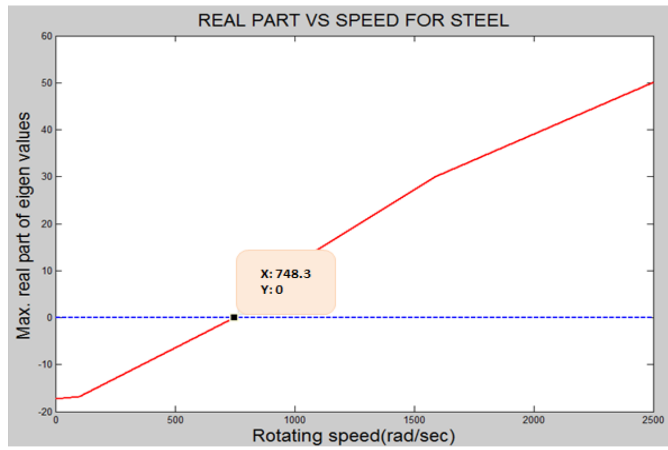

Figure 6. Stability diagram of conventional shaft.

From the stability results, it can be concluded that the maximum real part of the FG shaft surpasses that of the conventional shaft. The conventional shaft remains stable at speeds up to 748.32 rad/sec, while the FG shaft is stable at speeds up to 1034.65 rad/sec. Beyond these speeds, both systems become unstable. The FG shaft is better suited for higher speeds because of its enhanced stability**.**

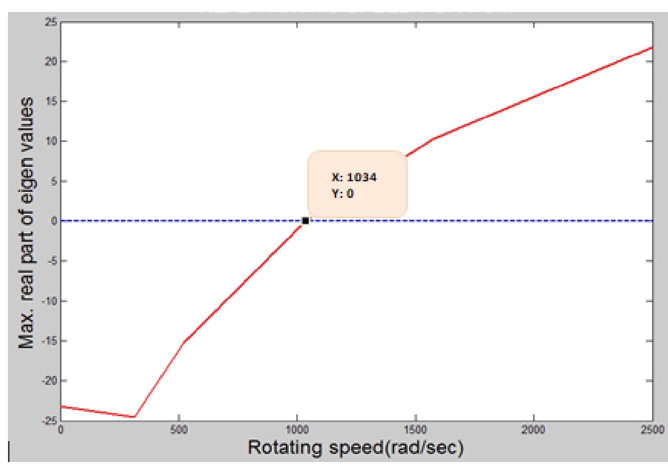

Figure 7. Stability diagram of FG shaft.

5. INFLUENCE OF GRADIENT INDEX ON UNBALANCE RESPONSE OF FG ROTOR

As the value of the gradient index increases, the magnitude of the unbalanced response of the FG shaft also increases, while the critical speeds and stability of the rotor system decrease. A summary of the effect of the gradient index is presented in Table 2.

Table 2. Effect of gradient index

Power law gradient	Unbalance response (µm)	Critical Speed in I Fwd mode (rad/s)	Speed (rad/s) real part's sign change
K=2	93.17	447.13	1034
K=5	95.24	431.2	978.1
K=10	98.38	419.89	951.4

6. DYNAMIC ANALYSIS OF FG SHAFT WITH SPRINGS

SMA springs which used in the system are made from Nitinol wire of diameter of 2.54 mm. In this examination, the bearing pedestal is held up by eight Nitinol springs, with four springs positioned horizontally and four springs oriented vertically. The transformation from austenite phase to Martensite phase occurs at 77 °C. The stiffness of the Nitinol spring has been estimated to be 533.33 N/m and 2430.98 N/m in deactivate and activate states[10] respectively.

7. UNBALANCE RESPONSE OF FG SHAFT IN DEACTIVATE AND ACTIVATED STATE OF NOTINOL SPRINGS

Figure 8 illustrates the unbalanced response of the FG rotor with springs in a deactivated state, while Fig. 9 depicts the unbalanced response in an activated state at 100°C.

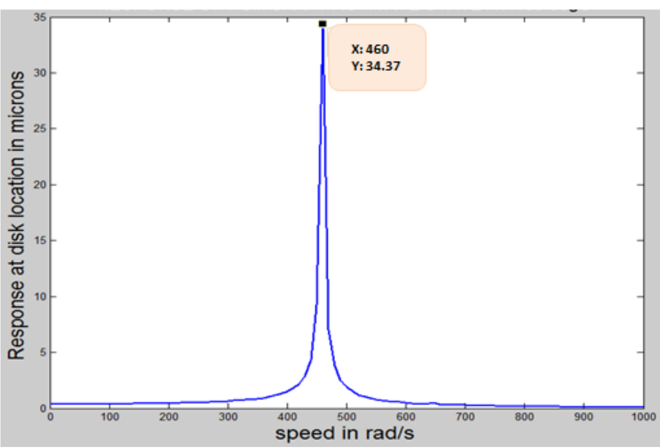

Figure 8. Unbalance response of FG Shaft with SMA supports in activate state.

In Fig. 8, in the activation state, the critical speed shifted to a higher value of 460 rad/sec, and the unbalanced response decreased to 34.37 µm at 100 °C. In Fig. 9, due to the deactivation state of the springs, the critical speed shifted to a lower value of 420 rad/sec.

The activation and deactivation strategy can be implemented in this system to control resonance by shifting the critical speeds. Consequently, the rotor is coasted up in the activated state of Nitinol springs and is brought past the critical speed of 420 rad/sec, which corresponds to the deactivated state of the springs. This approach helps avoid resonance

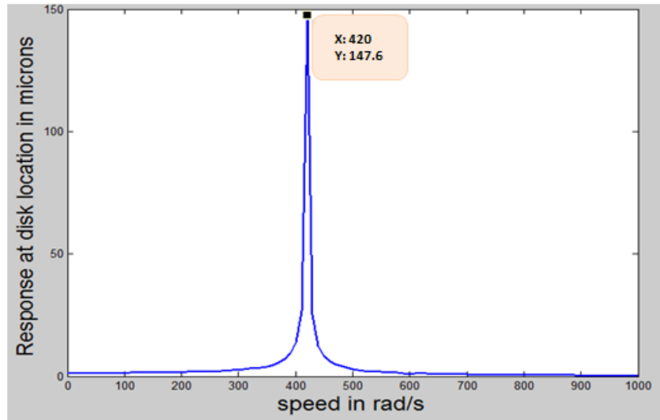

Figure 9. Unbalance response of FG shaft with SMA supports in deactivate state.

associated with the deactivated state. The deactivation of the springs occurs before reaching the critical speed of 460 rad/sec, which corresponds to the activated state of the springs, during the continued coast-up operation of the rotor system.

8. CAMPBELL DIAGRAM OF FG SHAFT WITH SMA SUPPORTS

Campbell diagram for the FG shaft with SMA supports in the activation state is shown in Fig. 10. The critical speed of this system is 452.17 rad/sec, while for the FG shaft, the critical speed occurs at 447.53 rad/s.

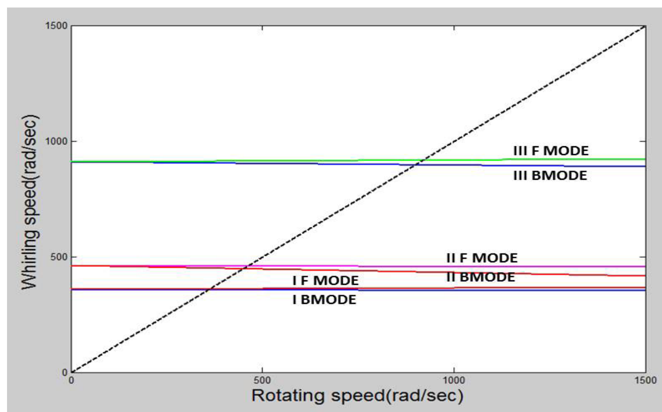

Figure 10. Campbell diagram of FG shaft with SMA supports.

9. CONCLUSIONS

The Power law gradient index (K) significantly influences the mechanical properties of FG materials. The variation of these properties is more affected by lower values of K than by higher values. The results indicate that the FG shaft is suitable for higher speeds with a lower magnitude of unbalanced response compared to conventional rotor systems in stable regions. Stability analysis shows that the FG shaft is more stable than the conventional rotor. The power law gradient index plays a crucial role in responses such as critical speeds, stability limits, and unbalanced responses derived from Campbell and stability diagrams. Comparative studies of various parameters of the FG shaft and conventional shaft indicate that the FG shaft results in a drastic increase in critical speed and stability, along with a significant reduction in amplitudes of unbalanced response when compared to the conventional rotor. However, the incorporation of Nitinol in the system leads to a marginal shift in critical speed and a lesser reduction in unbalanced response. Nevertheless, by employing an activation and deactivation strategy for Nitinol, resonance can be avoided by shifting the critical speed during the coast-up and coast-down operation of the rotor.

REFERENCES

1. Nelson, H.D. & Mc Vaughn, J.M. The dynamics of rotor-bearing systems using finite element method. *J. Engin. Industry*, 1976, **98**, 593–600.
2. Zorzi, E.S. & Nelson, H.D. Finite element simulation of rotor-bearing systems with internal damping. *J. Engin. Power*, 1977, **99**, 71-76.
3. Chang, M.Y.; Chen, J.K.; Chang, C.Y. A simple spinning laminated composite shaft model. *Int. J. Solids Struct.*, 2004 **41**, 637–662.
4. Koteswara, R. & Tarapada, Roy Vibration analysis of functionally graded rotating shaft system. *In* 12th International conference on vibration problems, ICOVP, 2015, **144**, 775-780.
5. Boukhalfa, A. Dynamic analysis of a spinning functionally graded material shaft by the p-version of the finite element method. *Latin Am. J. Solids and Struct.* 2014, **11**, 2018-2038.
   doi: 10.1590/S1679-78252014001100007.
6. Gupta, K.; Darpe, A.K.; Kumar, B.; Bhatia, A.; Ahmed, S.M.; Aravindhan, T.S. & Nakra, B.C. Resonance control of rotor using shape memory alloys. *Adv. in Vibration Engin.*, 2009, **8**(3), 239-246.
7. Enemark, S.; Ilmar, S. & Marcelo, A.S. Shape memory alloys applied to improve rotor-bearing system dynamics-an experimental investigation. *In* XVII International Symposium on Dynamic Problems of Mechanics. 2015.
8. Yong-Yong, H.; Oi, S.; Chu, Fu-Lei & Li, H.X. Vibration control of a rotor–bearing system using shape memory alloy: I. *Theory. Smart Materials and Struct.*, 2007, **16**, 122.
   doi: 10.1088/0964-1726/16/1/015
9. Gayen, D. & Roy, T. Finite element based vibration analysis of functionally graded spinning shaft system. Proceedings of the Institution of Mechanical Engineers, *Part C: J. Mech. Engin. Sci.*, 2014, **228**, 3306 - 3321.
10. Pelton, A.; DiCello, J. & Miyazaki; S. Optimisation of processing and properties of medical grade nitinol wire, *Min. Invas. Ther & Allied Technol.,* 2000, **9**(1),107–118

CONTRIBUTOR

Mr K. Udayanand obtained his M.Tech in Machine Design and Machine Dynamics from IIT, Chennai. Currently, he serves as a Scientist ‘D’ at DRDO-NSTL, Visakhapatnam. His specialisation include: Vibration and noise analysis, defect diagnosis, and condition monitoring of onboard machinery in ships, design and development of shells for underwater weapons and sub-systems.